Spatial Distribution of Serotonergic

Raphespinal Neurons in the Neonatal Mouse Brainstem

A Thesis

Presented to

The Academic Faculty

by

Luke Bumgardner

In Partial Fulfillment

of the Requirements for the Degree

Bachelor of Science in the

School of Biomedical Engineering

Georgia Institute of Technology & Emory School of Medicine

Perreault Laboratory

Luke Bumgardner

May 2019

Abstract

Descending serotonergic (5-HT) neurons located in the brainstem are known to influence mammalian locomotion. Neonates have poorer locomotor abilities than adults. Theoretically, a lesser contribution from 5-HT descending neurons in neonates is possible. However, a detailed quantification of 5-HT descending neurons in the neonate has yet to be performed. In this study, we quantify 5-HT descending neurons in each caudal raphe nuclei of the brainstem in the neonatal Pet1-GCaMP6 mouse (P1-P2). Descending 5-HT neurons were present in only three raphe nuclei, the raphe magnus (RMg), the raphe pallidus (RPa), and the raphe obscurus (ROB). Results show that 11% of all 5-HT neurons present in these nuclei project down the brainstem into the spinal cord. The largest majority of 5-HT descending neurons was found in the raphe pallidus (RPa), followed by the raphe magnus (RMg) nuclei, and finally, the raphe obscurus (ROB) nuclei. We discuss how these data compare with data obtained in adult animals.

Introduction

The involvement of descending serotonergic neurons in motor-related functions is well established, but their specific role remains largely unclear (Ballion et al., 2002; Cabaj et al., 2017). 5-HT neurons are found in nine nuclei spanning the dorsal, medial, and caudal raphe of the brainstem. The dorsal and medial raphe nuclei are known to innervate the forebrain, whereas the caudal raphe nuclei innervate both the brainstem and spinal cord. Substantial progress has been made to identify subclasses and projection patterns of 5-HT neurons in various mammals (Chiba & Masuko, 1989), including adult mice (Liang, et al., 2011; Liang et al., 2015; Okaty et al., 2015; Okaty et al., 2019). However the spatial distribution of the descending 5-HT neurons in the neonatal mouse brainstem is still not characterized. The experiments described in this report are part of a larger project designed to investigate the roles of 5-HT subpopulations and neural pathways on locomotor systems.

The project aims to analyze and quantify the distribution of descending 5-HT neurons across different raphe nuclei in the neonatal mouse, a model fruitfully used for studying descending motor systems (Siversten et al., 2016; Jean-Xavier & Perreault, 2018). Evidence shows 5-HT neurons play a role in locomotion in neonatal and adult rodents (Slawinska et al., 2014), therefore it is expected a substantial proportion of 5-HT neurons will be spinal-projecting neurons (Liu et al., 2009; Cabaj et al., 2017; Correia et al., 2017). We used pups obtained from crossbreeding Pet1-Cre mice (Scott et al., 2005) and GCaMP6 reporter mice (Madisen et al., 2015). To be able to distinguish 5-HT descending neurons from non-descending 5-HT neurons we applied a retrograde fluorescent tracer unilaterally to the cervical spinal cord.

Preliminary quantification of 5-HT neurons shows ipsilaterally descending neurons in the raphe magnus (RMg), raphe pallidus (RPa), and raphe obscurus nuclei (ROB), but no 5-HT descending neurons in the raphe interpositus (RIP) nucleus (Figure 1). Contralaterally descending neurons were observed, however these neurons were not quantified. The observed distribution of raphespinal descending neurons

in the neonatal mouse brainstem is compared to the raphespinal descending distribution in the adult mouse (VanderHorst & Ulfhake, 2006; Liang et al., 2011).
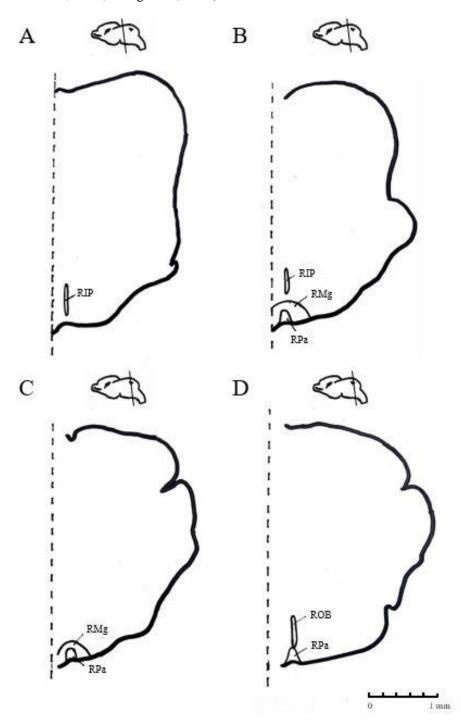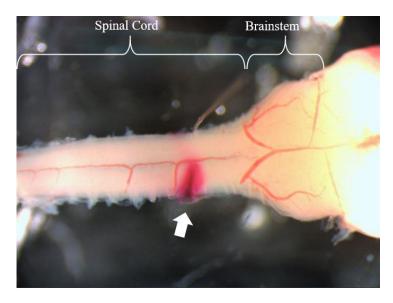

Figure 1. Transverse brainstem sections of the developing mouse brain representing caudal raphe nuclei of interest. Sections are ordered from rostral to caudal and mm values are measured caudally from the bregma. A) Section containing RIP (5.55 mm). B) Section containing RIP, RMg, and RPa (6.15 mm). C) Section containing RMg and RPa (6.63 mm). D) Section containing ROB and RPa (6.87 mm). Scale bar represents 1 mm. Adapted from Paxinos et al. 2007.

Procedures

Experimental Procedures

Experiments were performed on neonatal (postnatal day (P) 1-2) Pet1-Cre/GCaMP6 trans-heterozygous mice (n=5), where 5-HT neurons selectively express the green fluorescent protein GCaMP6. All animal protocols followed US National Institutes of Health guidelines and were approved by Emory University Institutional Animal Care and Use Committee.

Animals were anesthetized with isoflurane 4% and, after a craniotomy and a laminectomy, their brain stem-spinal cord was dissected out. Brain stem-spinal cords were then pinned down in a dissection chamber containing cold and oxygenated artificial cerebrospinal fluid (aCSF). As shown in Figure 2, the cervical spinal cord was hemisected and fluorescent tracer rhodamine dextran amine (RDA) was applied into the lesion. The tracer was taken up by the lesioned descending axons and transported to the soma of these neurons in the brain stem.

Figure 2. Crystals of RDA were applied into a hemisected lesion, indicated by a white arrow, made unilaterally at the cervical level of the spinal cord.

After 8 hours of labeling, samples were fixed in 4% paraformaldehyde overnight, and then moved to 30% sucrose for tissue osmotic equilibration. The spinal cord of each sample was then cut in the thoracic

region, well below the hemisection, and discarded. The brainstem and remaining spinal cord were then frozen using liquid nitrogen and cut in the transverse plane in order to obtain two series of alternating 30-μm-thick transverse sections. The sections from one of the two series underwent immunohistochemistry against GFP (anti-GFP) using both Abcam chicken polyclonal anti-GFP primary antibody (10 mg/mL) and Invitrogen Rabbit anti-tetramethylrhodamine primary antibody (1 mg/mL). Primary antibodies were used at a 0.4% v/v concentration. The remaining series was preserved as a back-up in the case the first series was damaged. All sections were mounted using a mounting medium containing the nuclear marker DAPI and cover-slipped.

Analysis

We used the spinal cord sections to verify the extent of the cervical lesion and crystal loading techniques of each of the samples. Next, we imaged the brainstem sections using a Keyence BZ-X fluorescent microscope. Images of all sections were acquired at 4x using the X-Y stitching feature of the Keyence software. Sections with dense 5-HT neuron localization were imaged at 20x. These sections were imaged at 20x using Z-plane image acquisition with optical sections of 1 μm. Z-stacks were used to verify co-localization of GFP and RDA in neurons. We used ImageJ software to count neurons in the RPa, RMg, ROB, and RIP. Only neurons containing DAPI staining were counted. We counted all 5-HT neurons (GFP+) and all descending 5-HT neurons (GFP+ co-localizing RDA+) in the caudal nuclei. We did not count descending non-5-HT neurons (RDA+ only). For each sample, we counted one of the two alternating series. Each series ranged from 35 to 50 sections per series. Counts were multiplied by two to reach a final neuron count for the series (half brain count). We used the Atlas of the Developing Mouse Brain (Paxinos et al., 2007) as a reference to plot observed neurons within raphe nuclei.

Results

Assessment of the RDA application sites revealed incomplete hemisections in two of the five brainstem-spinal cord samples (S4 and S5). The incompleteness of the hemisections in samples S4 and S5

was confirmed by finding only a few GFP+/RDA+ labelled neurons in each sample (13 and 19, respectively). Therefore, samples S4 and S5 were excluded from the analysis presented below.

In the three remaining samples S1-S3, the number of retrogradely labelled GFP+/RDA+ neurons were substantial, totaling 110 in S1, 91 in S2, and 166 in S3. We then looked at the specific distribution of GFP+/RDA+ neurons in the RPa, RMg, ROB, and RIP. The average numbers of RDA+ only neurons and GFP+/RDA+ neurons across samples S1-S3 are represented graphically in Figure 3 (see Table 1 in addendum for tabular representation). The largest number of GFP+/RDA+ neurons was found in the RMg and RPa (Figure 3). Figure 4 shows an example of the labeling obtained in the RPa nucleus of S3. Although RDA+ only neurons were not counted, a substantial number of neurons were observed in the caudal nuclei.
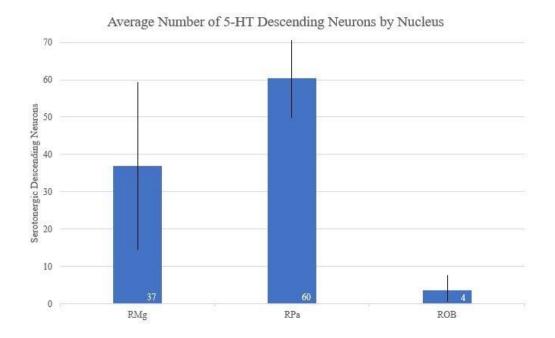
Figure 3. Bar graph displaying average number of serotonergic descending neurons (GFP+/RDA+) in caudal raphe nuclei across samples S1-S3. Error bars represent the standard deviation of serotonergic descending neurons for each nucleus.
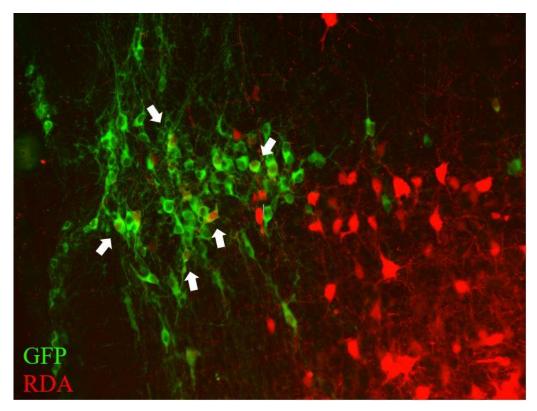

Figure 4. High magnification (20x) image of serotonergic descending neurons (GFP+/RDA+) in the RPa of S3. GFP-expressing neurons are serotonergic neurons, RDA labelled neurons are descending neurons, and double labelled neurons indicated with white arrows are serotonergic descending neurons.

Discussion

This work quantifies, for the first time, 5-HT neurons of caudal raphe nuclei in neonatal mice. More significantly, the quantification of 5-HT neurons, in combination with RDA labeling of descending neurons in the brainstem, allows for the identification of raphespinal 5-HT neurons that project to the spinal cord. Results show that 11% of all 5-HT neurons in the caudal brainstem project down the brainstem to the spinal cord. The location and distribution of 5-HT descending neurons are compared to results in adult mice reported by Liang et al. (2011) who used Fluoro-Gold and horseradish peroxide to retrogradely label ipsilateral descending neurons in the mouse brain and brainstem. The authors counted every seventh 40 μm section and scaled the count to the total number of sections in order to estimate the total absolute number of neurons. They reported absolute descending neuron counts in two different samples across various regions including: 921 descending neurons in the RMg, 431 descending neurons in the RPa, 358 descending neurons in the ROB, and 283 descending neurons in the RIP. Similar to our observations, the authors noted a substantial number of descending neurons within the caudal raphe nuclei. Based on our results we would suggest that most of these descending neurons are not 5-HT descending neurons. Interestingly, the authors noted descending neurons in the RIP. We failed to see descending 5-HT neurons in the RIP, indicating descending neurons in the RIP may be of a different transmitter phenotype. Liang et al. (2011) also noted possible labeling contamination to the contralateral side. Therefore, an alternative explanation is that RIP descending neurons are contra-projecting. However further exploration would be needed to test between all these possibilities. The location and distribution of 5-HT descending neurons were also compared to results in adult mice reported by VanderHorst & Ulhfake (2006). Similar to our results, the authors observed descending 5-HT neurons in the RMg, RPa, and ROB. They also found no descending 5-HT neurons present in the RIP.

Technical considerations

GFP+/RDA+ neurons were present in only three of the five samples, underlying the importance of analyzing and verifying RDA labeling effectiveness and techniques after each experiment. The absence of

GFP+/RDA+ neurons in S4 and S5 could be attributed to improper lesioning and/or insufficient RDA loading. A common issue with retrograde labeling is gauging and inserting the proper amount of crystal to ensure complete labeling occurs. As additional samples are analyzed, it will become imperative to compare RDA labeled neuron distributions along the brainstem to ensure consistency of labeling.

Considerations for continuation of the work in the future

It is imperative that additional samples are analyzed to improve effect size and allow for comparative statistical analysis. Aside from accumulating additional samples, it would be interesting in future work to study the spatial distribution of 5-HT axons within the white matter of the spinal cord. This would be informative in relation to spinal cord injury at an early age. The number of GFP+/RDA+ neurons present in the caudal nuclei was surprisingly low (11%), however this may be explained by the use of neonatal mice. We found a substantial number of RDA+ only neurons in the caudal raphe nuclei; it may be possible these descending neurons also contribute to locomotion. Although the counting of these RDA+ only neurons was initially outside the scope of the project, in future studies it would be interesting to determine the transmitter phenotype of these neurons. As this work is the first to quantify the 5-HT neuron distribution of caudal raphe nuclei in neonatal mice, ideally, field experts and future researchers will use the quantification to further explore the specific roles of these neurons during motor activity in neonates.

References

Ballion, Berangere, Pascal Branchereau, Jacqueline Chapron, Denise Viala (2002). "Ontogeny of descending serotonergic innervation and evidence for intraspinal 5-HT neurons in the mouse spinal cord." *Developmental Brain Research* 137: 81-88.

Cabaj, Anna M., Henryk Majczynski, Erika Couto, Phillip F. Gardiner, Katinka Stecina, Urszula Sławinska, Larry M. Jordan (2017). "Serotonin controls initiation of locomotion and afferent modulation of coordination via 5-HT receptors in adult rats." *Journal of Physiology* 595.1: 301-320.

Chiba T., and Masuko S. (1989). "Coexistence of varying combinations of neuropeptides with 5-hydroxytryptamine in neurons of the raphe pallidus et obscurus projecting to the spinal cord." *Neuroscience Research* 7(1): 13–23.

Correia, Patrícia, Eran Lottem, Dhruba Banerjee, Ana Machado, Meagn Carey, and Zachary Mainen (2017). Transient inhibition and long-term facilitation of locomotion by phasic optogenetic activation of serotonin neurons. *eLife* 6:10.7554/eLife.20975.

Jean-Xavier C., and Perreault M-C (2018). "Influence of Brain Stem on Axial and Hindlimb Spinal Locomotor Rhythm Generating Circuits of the Neonatal Mouse." *Frontier Neuroscience* 12: 53.

Liu, T. A., Peter B. Hedlund, Keir G. Pearson, Larry M. Jordan (2009). "Spinal 5-HT7 receptors are critical for alternating activity during locomotion: in vitro neonatal and in vivo adult studies using 5-HT7 receptor knockout mice." *Journal of Neurophysiology* 102: 337-348.

Liang, Huazheng, George Paxinos, Charles Watson (2011). "Projections from the brain to the spinal cord in the mouse." *Brain Structure and Function* 215: 159-186.

Liang, Huazheng, Shaoshi Wang, Richard Francis, Renee Whan, Charles Watson, George Paxinos (2015). "Distribution of raphespinal fibers in the mouse spinal cord." *Molecular Pain* 11: 42.

Okaty, B.W., Commons, K.G., Dymecki, S.M. (2019). "Embracing diversity in the 5-HT neuronal system." *Nature Reviews Neuroscience*.

Okaty, B.W., Freret, M.E., Rood, B.D., Brust, R.D., Hennessy, M.L., deBairos, D., Kim, J.C., Cook, M.N., Dymecki, S.M. (2015). "Multi-scale molecular deconstruction of the serotonin neuron system." *Neuron* 88(4): 774–791.

Paxinos, George, Glenda Margaret Halliday, Charles Watson, Yuri Koutcherov, Hongquin Wang (2007). "Atlas of the Developing Mouse Brain at E17.5, P0 and P6."

Scott, Michael, Christi Wylie, Jessica Lerch, RoxAnne Murphy, Katherine Lobur, Stefan Herlize, Weihong Jiang, Ron Conlon, Ben Strowbridge, Evan Deneris (2005). "A genetic approach to access serotonin neurons for in vivo and in vitro studies" *Proceedings of the National Academy of Sciences of the United States of America* 102: 16472-16477.

Sivertsen MS, Perreault M-C, Glover JC (2016) "Pontine reticulospinal projections in the neonatal mouse: Internal organization and axon trajectories." Journal of Comparative Neurology 524:1270-1291.

Sławińska, U., Miazga, K., & Jordan, L. M. (2014). "5-HT$_2$ and 5-HT$_7$ receptor agonists facilitate plantar stepping in chronic spinal rats through actions on different populations of spinal neurons." *Frontiers in Neural Circuits* 8: 95.

VanderHorst, V.G.J.M., & Ulfhake, B. (2006). "The organization of the brainstem and spinal cord of the mouse: relationships between monoaminergic, cholinergic, and spinal projection systems." *Journal of Chemical Neuroanatomy* 31: 2-36.

Addendum

Table 1. Number of non-descending and descending ($\downarrow$) serotonergic neurons in caudal raphe nuclei across S1-3.

Nucleus	S1		S2		S3		Average	
	5-HT	5-HT $\downarrow$	5-HT	5-HT $\downarrow$	5-HT	5-HT $\downarrow$	5-HT	5-HT $\downarrow$
RMg	482	11	695	36	497	64	558 ± 97	37 ± 22
RPa	887	59	637	48	636	74	720 ± 118	60 ± 11
ROB	303	8	308	0	329	3	313 ± 11	4 ± 3
RIP	31	0	24	0	17	0	24 ± 5	0 ± 0
Total	**1,703**	**78**	**1,664**	**84**	**1,479**	**141**	**404 ± 58**	**25 ± 9**